International Journal of Biological Macromolecules 265 (2024) 130806

Contents lists available at ScienceDirect

International Journal of Biological Macromolecules

journal homepage: www.elsevier.com/locate/ijbiomac

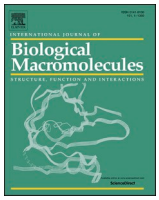

A generalizable reactive blending strategy to construct flame-retardant, mechanically-strong and toughened poly(L-lactic acid) bioplastics

Zimeng Zhang [a], Siqi Huo [b,c,*], Lingfeng Yu [a], Guofeng Ye [a], Cheng Wang [a], Qi Zhang [a], Zhitian Liu [a,**]

[a] Hubei Engineering Technology Research Center of Optoelectronic and New Energy Materials, School of Materials Science & Engineering, Wuhan Institute of Technology, Wuhan 430205, China
[b] Centre for Future Materials, University of Southern Queensland, Springfield 4300, Australia
[c] School of Engineering, University of Southern Queensland, Springfield Central 4300, Australia

ARTICLE INFO

Keywords:
Poly(L-lactic acid)
Flame Retardancy
Mechanical properties

ABSTRACT

Poly(L-lactic acid) (PLA) is an environmentally-friendly bioplastic with high mechanical strength, but suffers from inherent flammability and poor toughness. Many tougheners have been reported for PLA, but their synthesis usually involves organic solvents, and they tend to dramatically reduce the mechanical strength and cannot settle the flammability matter. Herein, we develop strong, tough, and flame-retardant PLA composites by reactive blending PLA, 6-((double (2-hydroxyethyl) amino) methyl) dibenzo [c, e] [1,2] oxyphosphate acid 6-oxide (DHDP) and diphenylmethane diisocyanate (MDI) and define it PLA/xGH, where x indicates that the molar ratio of -NCO group in MDI to -OH group in PLA and DHDP is 1.0x: 1. This fabrication requires no solvents. PLA/2GH with a -NCO/-OH molar ratio of 1.02: 1 maintains high tensile strength of 63.0 MPa and achieves a 23.4 % increase in impact strength compared to PLA due to the incorporation of rigid polyurethane chain segment. The vertical combustion (UL-94) classification and limiting oxygen index (LOI) of PLA/2GH reaches V-0 and 29.8 %, respectively, because DHDP and MDI function in gas and condensed phases. This study displays a generalizable strategy to create flame-retardant bioplastics with great mechanical performances by the *in-situ* formation of P/N-containing polyurethane segment within PLA.

1. Introduction

With the increasingly serious problem of microplastics pollution, substantial efforts have been invested to the development of biodegradable bioplastics. Among them, PLA has been widely utilized in the industries of packaging, furniture, electronics, and electrical equipment because of its good biocompatibility, high mechanical strength, and ease of processability. However, the intrinsic flammability and poor toughness of PLA limit its potential application in high-end industries [1–3].

Blending with toughening agents is an economical and convenient way to improve the toughness of PLA [4]. In recent years, some inorganic nanofillers proved to be effective in improving the mechanical performances of PLA, *e.g.,* carbon nanotubes [5,6], and bamboo cellulose nanowhisker (BCNW) [7–9]. Flexible plastics and compatibilizers, *e.g.,* poly (butylene succinate) (PBS) [10], and polycaprolactone (PCL) [11], also possess a toughening effect towards PLA. At the same time, some renewable vegetable oils have attracted wide attention in toughening PLA because they are cost-effective and bio-based [12–18]. However, due to the differences in polarity, most of these toughening agents and PLA are incompatible, resulting in poor interface bonding force and unsatisfied toughening effect. Reactive blending is an effective method to enhance the interface bonding force and thus compatibility between PLA and additives *in-situ* [19–21]. Hence, this method is widely applied in the fabrication of high-performance, tough PLA composites [22–24]. Obviously, *in-situ* forming polyurethane (PU) [25,26] or polyamide (PA) [27] elastomers within the PLA matrix by reactive blending contributes to improving the toughness and maintaining the mechanical robustness. However, this kind of modification cannot address the flammability issue of PLA, which is also another critical factor restricting the high-performance application of PLA. Although adding flame retardants can enhance the fire retardancy, most of them will catalyze the depolymerization of PLA and thus reduce the

* Correspondence to: Centre for Future Materials, University of Southern Queensland, Springfield 4300, Australia.
** Corresponding author.
E-mail addresses: Siqi.Huo@unisq.edu.au, sqhuo@hotmail.com (S. Huo), able.ztliu@wit.edu.cn (Z. Liu).

https://doi.org/10.1016/j.ijbiomac.2024.130806
Received 11 December 2023; Received in revised form 18 February 2024; Accepted 10 March 2024
Available online 13 March 2024

mechanical performances [28,29]. Hence, it is a great challenge to break the trade-off of flame retardancy and mechanical performances for PLA.

PU elastomer is a typical segmented block copolymer, which is fabricated by the polyaddition reaction between polyol and diisocyanate [21,30]. Due to the diversity of polyol and diisocyanate, the performances of PU elastomer are highly tunable [31,32]. To accommodate the sustainable development strategy, the environmentally-friendly phosphorus (P)- and nitrogen (N)-derived flame retardants are widely utilized in polymeric materials [33–37]. Obviously, using P-containing diols as raw materials can obtain the intrinsic flame-retardant P/N-containing PU elastomers [38,39]. Based on the above analyses, we assume that constructing P/N-containing PU chain segment in PLA *in-situ* by reactive blending is a promising approach to address the flammability and toughness issues of PLA.

In this study, the flame-retardant, robust, and tough PLA/GH composites were fabricated through simple reactive blending of PLA and commercially available DHDP and MDI without the usage of any solvents. Our results confirm that the as-prepared PLA/2GH composite achieves good mechanical properties, with a tensile strength of 63.0 MPa and 23.4 % and 14.4 % enhancements in the impact strength and elongation at break relative to those of PLA. Moreover, this composite also passes a UL-94 V-0 classification and a high limiting oxygen index of 29.8 %, with remarkable decreases in peak heat release rate (PHRR) and total heat release (THR), demonstrating that it can be classified into a self-extinguishing material (UL-94 V-0 rating and LOI $\geq$ 28.0 %). Thereby, this work outlines a facile fabrication method for the high-performance, fire-safe bioplastics by simple reactive blending with phosphorus-containing diol and nitrogen-containing diisocyanate.

2. Experimental section

2.1. Materials

Poly(L-lactic acid) (3052D) was purchased from Nature-Works LLC (USA), and its number-average molecular weight (M_n) was ~37,000 g/mol. 6- ((Double (2-hydroxyethyl) amino) methyl) dibenzo [c, e] [1,2] oxyphosphate acid 6-oxide (DHDP, AR) was purchased from Henan Tianfu Chemical Co., Ltd. (China). Diphenylmethane diisocyanate (MDI, AR) was supplied by Shanghai Energy Chemical Co., Ltd. (China). All chemicals were applied as received.

2.2. Fabrication of PLA composites

The dried PLA was introduced into a torque rheometer and blended at 180 °C and 70 rpm for 3 min to melt, and MDI was added into the chamber and blended for about 10 min to react with the PLA matrix. DHDP was then introduced and blended for another 10 min. The gained mixture was cooled to room temperature, and then hot pressed at 170 °C and 16 MPa to obtain the MDI/DHDP-containing PLA specimen. The loading level of DHDP was fixed at 20 wt%. The obtained MDI/DHDP-containing PLA sample is named as PLA/xGH, where x demonstrates that the molar ratio of -NCO group in MDI to -OH group in PLA and DHDP is 1.0x: 1. For instance, PLA/1GH represents the MDI/DHDP-containing PLA sample with a -NCO: -OH molar ratio of 1.01: 1. The PLA containing 20 wt% of DHDP (PLA/20DHDP) was prepared by the above method without the addition of MDI. The PLA/MDI (mass ratio: 64.1 g: 15.9 g) composite was also fabricated to investigate the interphase reaction between PLA and MDI. Detailed formation is shown in Table 1.

2.3. Characterization

Fourier transform infrared (FTIR) spectra were recorded on a Nicolet 6700 spectrometer (USA) from 500 to 4000 cm^{-1} by the KBr pelleting method. The micro-morphology of specimen was investigated using a JSW-5510LV scanning electron microscopy (SEM, Japan).

Table 1
The formulations of PLA composites.

Sample	PLA (wt %)	DHDP (wt %)	MDI (wt %)	N content (%)	P content (%)	Molar ratio of -NCO and -OH
PLA	100	0	0	0	0	0
PLA/DHDP	80	20	0	0.84	1.86	0
PLA/1GH	64.4	20	15.6	2.59	1.86	1.01:1
PLA/2GH	64.2	20	15.8	2.61	1.86	1.02:1
PLA/3GH	64.1	20	15.9	2.62	1.86	1.03:1

Based on ASTM D638 and D790, a SHK-A104 equipment (Hengke, China) was applied to conduct the tensile and flexural tests at the speed of 5.0 mm/min. According to GB/T 1843-2008, an impact apparatus (LIANXIANG, China) was utilized to carry out the impact test. Five specimens were tested for each component to ensure the reliability of experimental data. Thermogravimetric analysis (TGA) was carried out by a NETZSCH STA449F3 equipment (Germany) from 25 to 800 °C in nitrogen condition, and the ramp-up was 20 °C/min. The temperature at 5 % weight loss ($T_{5\%}$), temperature at the maximum weight loss rate (T_{max}) and char yield at 800 °C (Y_c) were recorded. The powder sample (mass: ~8 mg) was used in this test.

In accordance with ASTM D2863 and D3801, the Jiangning JF-3 apparatus (China) was applied to investigate the LOI values of PLA samples (size: 100 mm × 6.5 mm × 3.0 mm), and the Jiangning CFZ-3 equipment (China) was used to evaluate the UL-94 classifications of PLA samples (size: 120 mm × 13 mm × 3.0 mm). Based on ISO 5660, the combustion behaviors of different samples (size: 100 mm × 100 mm × 3 mm) were studied on a VOUCH 6810 cone calorimeter (China) under a flux of 35 kW/m. The degrees of graphitization for chars were investigated on a Thermo Scientific DXR Raman microscope (USA) using 532 nm laser light. X-ray photoelectron (XPS) spectra of different samples were recorded by using a Thermo Scientific ESCALAB XI+ spectrometer (USA) under Al Ka radiation. Thermogravimetric analysis-infrared spectrometry (TGA-IR) was carried out by NETZSCH TG209F3 and TENSOR 27 apparatuses (Germany) from 25 to 800 °C under nitrogen atmosphere, and the ramp was 20 °C/min. The powder sample (mass: ~8.0 mg) was used in TGA-IR test. Pyrolysis gas chromatography/mass spectrometry (Py-GC/MS) was performed on a 5200+ lyator (CDS, USA) connected to the CLARUS SQ 8 T system (PerkinElmer, USA). The injector temperature is 250 °C; hold at 50 °C for 1 min and then rise to 280 at a rate of 5 °C/min. The GC/MS interface temperature was 280 °C, and the pyrolysis temperature was set to 500 °C.

3. Results and discussion

3.1. Interphase reaction

The *in-situ* reactions between PLA, DHDP and MDI during melt-blending are shown in Fig. 1a. The FTIR spectra of PLA/3GH, PLA/MDI, DHDP, MDI and PLA are presented in Fig. 1b. Obviously, the -NCO group in MDI is very reactive and easy to react with hydroxyl, carboxyl and amine groups [25]. In the FTIR spectrum of PLA/3GH, two absorption peaks at 1597 and 1533 cm^{-1} belong to the conjugated double bond and carbamate group, respectively, indicating that -NCO group in MDI has reacted with -OH groups in PLA and DHDP. The characteristic peaks at 1240 and 1058 cm^{-1} are assigned to the vibrations of P═O and O-P═O structures, suggesting the presence of DHDP. Notably, the absorption peak of -NCO at 2280 cm^{-1} can be found in the FTIR spectra of MDI and PLA/MDI, but it disappears in the FTIR spectrum of PLA/3GH, further demonstrating that MDI has completely reacted with PLA and DHDP during the preparation of PLA/3GH.

The torque as a function of time during melt-blending of PLA/3GH is shown in Fig. 1c. Adding MDI results in rapidly reduced and then

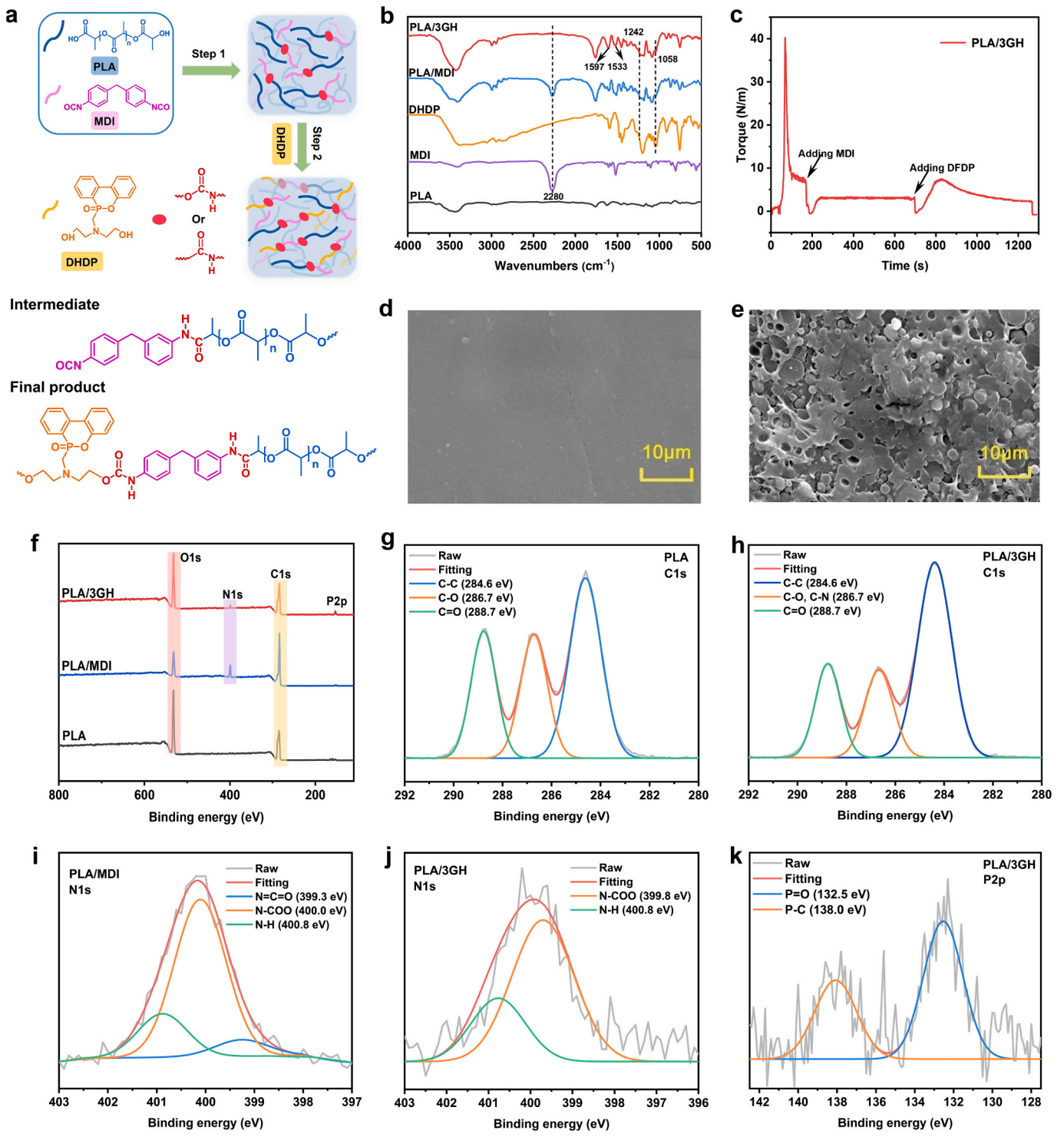

Fig. 1. (a) Schematic for the preparation of PLA/GH bioplastics, and chemical structures of intermediate and final PLA/GH; (b) FTIR spectra of PLA, DHDP, MDI, PLA/MDI and PLA/3GH; (c) torque variation during the melt blending process of PLA/3GH; SEM photos of (d) PLA and (e) PLA/3GH surfaces; (f) XPS full-scan spectra of PLA, PLA/MDI and PLA/3G; high-resolution XPS C1s spectra of (g) PLA, and (h) PLA/3GH; high-resolution XPS N1s spectra of (i) PLA/MDI, and (j) PLA/3GH; and (k) high-resolution XPS P2p spectrum of PLA/3GH.

increased torque because of the reaction between -NCO group of MDI and -OH group of PLA. As DHDP is introduced, the torque tends to equilibrium after rapidly increasing, which clearly indicates that the remained -NCO group of MDI reacts with -OH group of DHDP, leading to the increased viscosity of the whole system. The SEM images of PLA and PLA/3GH surfaces are displayed in Fig. 1d and e. The untreated PLA exhibits a smooth surface, while the PLA/3GH composite has a rough surface with some pores, further demonstrating that the interfacial reaction between PLA, MDI and DHDP has been conducted.

The chemical compositions and bonding states of PLA, PLA/MDI and PLA/3GH were analyzed by XPS, with the relevant spectra and data presented in Fig. 1f-k and S1 and Table S1. PLA/3GH contains carbon, oxygen, nitrogen, and phosphorus elements, further confirming the existence of MDI and DHDP (see Fig. 1f and Table S1). As presented in

Fig. 1g, h and S1a, the C—C, C-O/N and C═O peaks can be found in the high-resolution XPS C1s spectra of PLA, PLA/MDI and PLA/3GH. Notably, the introduction of benzene-rich MDI and DHDP results in an increased C—C peak intensity. In the XPS O1s spectra (see Fig. S1b-d), both O=C/P and O-C/P peaks appear at 531.9 and 532.5 eV, respectively. The N-COO and N—H peaks in the N1s spectrum of PLA/MDI demonstrates the reaction between MDI and PLA (see Fig. 1i), and the N=C=O peak cannot be found in the N1s spectrum of PLA/3GH (see Fig. 1j), indicating that DHDP has been chemically linked to the PLA/MDI matrix. In Fig. 1k, the P═O and P—C peaks further prove the existence of DHDP. Hence, the above analyses indicate that the PLA/GH composite is successfully prepared based on the interphase reaction of PLA, MDI and DHDP.

3.2. Mechanical performances of PLA and its composites

The mechanical properties of PLA, PLA/20DHDP and PLA/GH composites were compared to determine the necessity of covalently linking DHDP and MDI to PLA. As shown in Fig. 2a-c and Table S2, the elongation at break, tensile strength, impact strength, and flexural strength of PLA are 5.36 %, 64.1 MPa, 3.16 kJ/m^2, and 86.3 MPa, respectively. Adding 20 wt% of DHDP dramatically decreases the mechanical properties of PLA/20DHDP, of which the elongation at break, tensile strength, impact strength, and flexural strength are only 0.92 %, 18.7 MPa, 1.93 kJ/m^2, and 21.9 MPa. This is probably because the hydroxyl group in DHDP catalyzes the depolymerization of PLA during the melt-blending procedure [40,41]. As expected, the *in-situ* reacting strategy effectively maintains or even enhances the mechanical properties of PLA. As the molar ratio of -NCO and -OH reaches 1.02: 1, the elongation at break, tensile strength, impact strength, and flexural strength of as-fabricated PLA/2GH composite are 6.13 %, 63.0 MPa, 3.90 kJ/m^2, and 90.5 MPa, respectively. Compared with PLA, the elongation at break, impact strength, and flexural strength of PLA/2GH increase by 14.4 %, 23.4 %, and 4.9 %. Obviously, the PLA/2GH composite shows well-preserved mechanical robustness and enhanced toughness due to the *in-situ* formation of rigid polyurethane (PU) segment within the PLA matrix, which can absorb part of energy when the composite is subjected to the external forces and thus improve the toughness [25,42]. When the -NCO and -OH molar ratio further increases to 1.03: 1, the mechanical performances of PLA/3GH composite deteriorate, which may be due to the excess unreacted -NCO groups catalyzing the depolymerization of PLA. However, the mechanical performances of PLA/3GH composite are still much better than those of PLA/20DHDP composite. All these results demonstrate that covalently introducing rigid PU chain segment into PLA by using MDI and DHDP as raw materials are capable of effectively maintaining the mechanical robustness and enhancing the toughness.

To investigate the dispersion and toughening mechanism of the formed PU, the cross-sections of PLA and its composites after the notched Izod impact tests were analyzed *via* SEM. Based on the 'silver-shear band' theory, the well-dispersed PU is able to serve as the stress concentration site to form shear bands, microcracks and stripes to consume a lot of energy under external forces, hence enhancing the toughness of PLA [43]. As expected, the PLA/GH composites display much coarser cross-sections than virgin PLA (see Fig. 2d-g). Notably, many microcracks and shear bands can be detected within the cross-section of PLA/2GH composite, but it is hard to find the shear bands in the fractured surface of PLA/3GH composite. In sum, the uniformly dispersed, rigid PU chain segment can be formed within the PLA matrix under the appropriate molar ratio of -NCO to -OH (approximately 1.02: 1), which contributes to the dissipation of energy and thus toughness enhancement [26,42].

3.3. Thermal stability of PLA and its composites

The thermogravimetric analyses of PLA samples under nitrogen

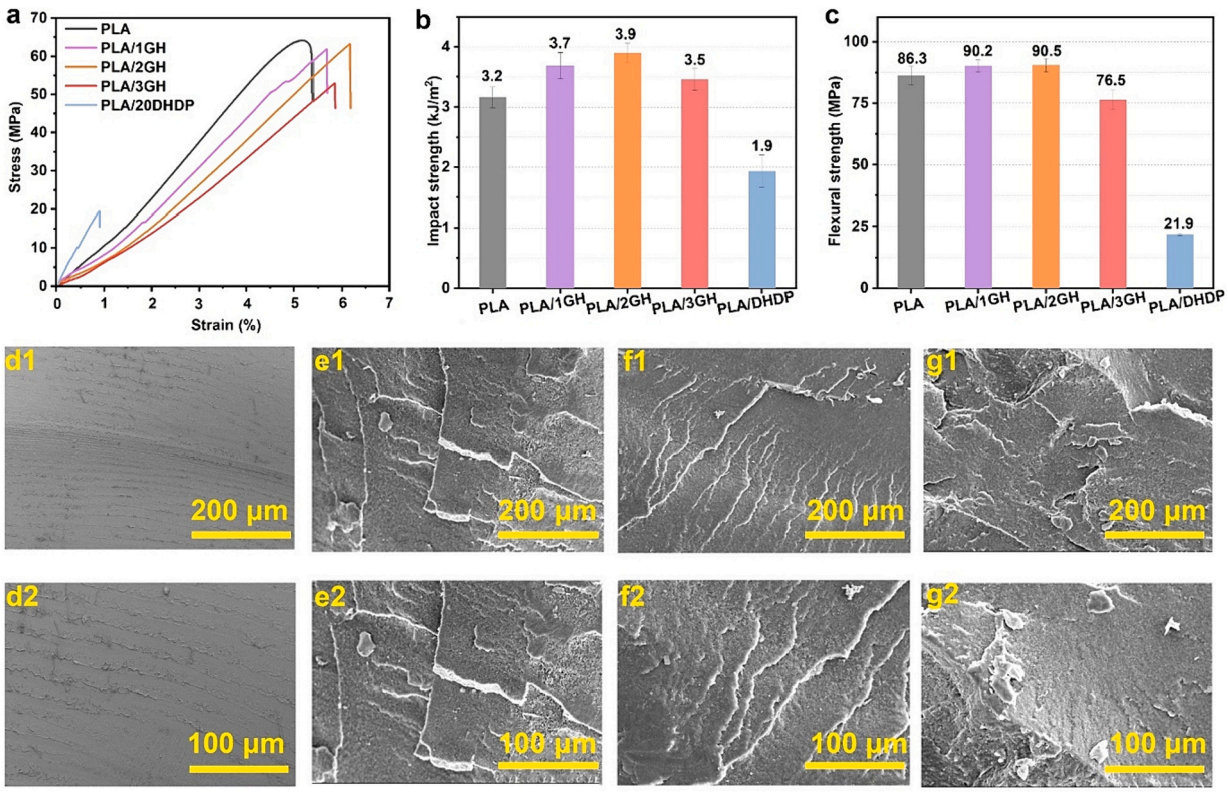

Fig. 2. (a) Tensile stress *vs.* strain plots of PLA and its composites; (b) impact strengths of PLA and its composites; (c) flexural strengths of PLA and its composites; and SEM photographs of for (d1, d2) PLA, (e1, e2) PLA/1GH, (f1, f2) PLA/2GH, and (g1, g2) PLA/3GH after the notched Izod impact tests under different magnifications.

atmosphere were conducted. The TG and derivative TG (DTG) plots and characteristic parameters are recorded in Fig. 3 and Table S3. The $T_{5\%}$ of PLA is 372 °C. When the MDI and DHDP are introduced, the $T_{5\%}$ values of PLA/GH composites reduce relative to that of PLA (see Fig. 3a and Table S3). For example, the $T_{5\%}$ values of PLA/2GH and PLA/3GH composites decrease to 321 and 318 °C, respectively, which is mainly because of the catalytic degradation of phosphorus-derived group in DHDP [37,44]. Similarly, the inclusion of DHDP also brings about the reduced T_{max} of PLA/GH composites relative to pure PLA (see Fig. 3b and Table S3), further manifesting that DHDP promotes the decomposition of PLA. The neat PLA leaves no char after the thermogravimetric test, while the Y_c values of PLA/GH composites are significantly enhanced. For instance, the Y_c of PLA/1GH composite reaches 9.8 %. Thereby, incorporating MDI and DHDP enhances the carbonization ability of PLA, which demonstrates the enhanced fire safety to a certain extent.

3.4. Flame retardancy of PLA and its composites

Table 2 displays the LOI values and UL-94 classifications of PLA and PLA/GH. Once ignited in air, pure PLA burns violently and generates a great deal of molten droplets continuously, thereby it cannot pass the vertical burning test, and its LOI is only 19.5 %. By *in-situ* reacting with MDI and DHDP, the LOI value and UL-94 level of PLA/GH increase significantly. For example, the LOI of PLA/1GH composite increases to 28.3 %, and that of PLA/3GH composite reaches 30.4 %. Moreover, the burning time of PLA/GH composites reduces with increasing -NCO/-OH molar ratio during the UL-94 tests, and all composites achieve the UL-94 V-0 rating. The covalent introduction of MDI and DHDP endows PLA with significantly enhanced fire safety. The mechanical and flame-retardant properties of PLA/2GH and previous flame-retardant PLA samples were compared in Fig. S2 and Table S4. In comparison to its counterparts, our PLA/2GH shows comparable tensile strength, and higher LOI value and impact strength enhancement, indicative of its improved mechanical and flame-retardant performances. Thus, the reactive blending strategy can effectively address the trade-off between flame retardancy and mechanical properties of PLA.

Cone calorimeter is widely utilized to evaluate the fire safety of polymers [45,46]. The cone calorimetry of PLA and PLA/GH composites was carried out, with the results revealed in Fig. 4 and Table S5. Like many previously-reported phosphorus-containing PLA systems, the PLA/GH composites display the reduced time of ignition (TTI) because DHDP catalyzes the decomposition of the matrix (see Table S5) [2,47–49]. The PLA/GH composites generate lower heat than PLA

Table 2
LOI and UL-94 data of PLA and its composites.

Sample	LOI (%)	UL-94 (3.2 mm)			
		$t_1 + t_2$[a] (s)	Dripping	Cotton ignition	Rating
PLA	19.5	>50	Yes	Yes	NR
PLA/1GH	28.3	4.6	Yes	No	V-0
PLA/2GH	29.8	3.3	Yes	No	V-0
PLA/3GH	30.4	1.6	Yes	N	V-0

[a] t_1, t_2 refer to average burning time after the first and second application of flame.

during cone calorimetry tests (see Fig. 4a and b and Table S5). For example, the PHRR and THR of PLA/3GH composite reduce from 474 kW/m^2 and 74.9 MJ/m^2 of PLA to 433 kW/m^2 and 42.2 MJ/m^2, by 8.6 % and 43.7 %. Similar decreases can also be detected in the PHRR and THR of other PLA/GH composites. The char yields and structures of PLA/GH composites are improved compared with those of PLA. In Fig. 4d-g, there is no char after the combustion of PLA, while all PLA/GH char layers show integrated surfaces and intumescent structures, of which the heights reach approximately 40 mm. The generation of such char layers contributes to retarding the heat release and oxygen permeation and protecting the matrix, thereby enhancing flame retardancy. The PLA/GH composites also present reduced degrees of gas-phase combustion compared with PLA, which is reflected by their lower average effective heat of combustion (AEHC, see Table S5). The reduced gas-phase combustion can also be confirmed by the increased average CO yield (ACOY, reflecting incomplete combustion) and decreased average CO_2 yield (ACO_2Y, reflecting complete combustion). Moreover, due to the gas-phase effects of DHDP and MDI, the total smoke release (TSR) values of PLA/GH composites are higher than that of PLA. These results suggest that the PLA/GH composites show superior fire retardancy to PLA due to the formation of expanded char layers and the suppression of gas-phase combustion.

3.5. Char residue analysis

The SEM photos of both PLA/2GH and PLA/3GH residue surfaces are exhibited in Fig. 5a and b. Obviously, both char layers are continuous and integrated with no obvious crack, thus it can isolate the diffusion of combustible gas and heat to retard the combustion reaction.

To further analyze the char layers of PLA/GH composites, the Raman spectroscopy was utilized. In the Raman spectra, the D and G bands at 1360 and 1580 cm^{-1} represent the disordered carbon and graphitized

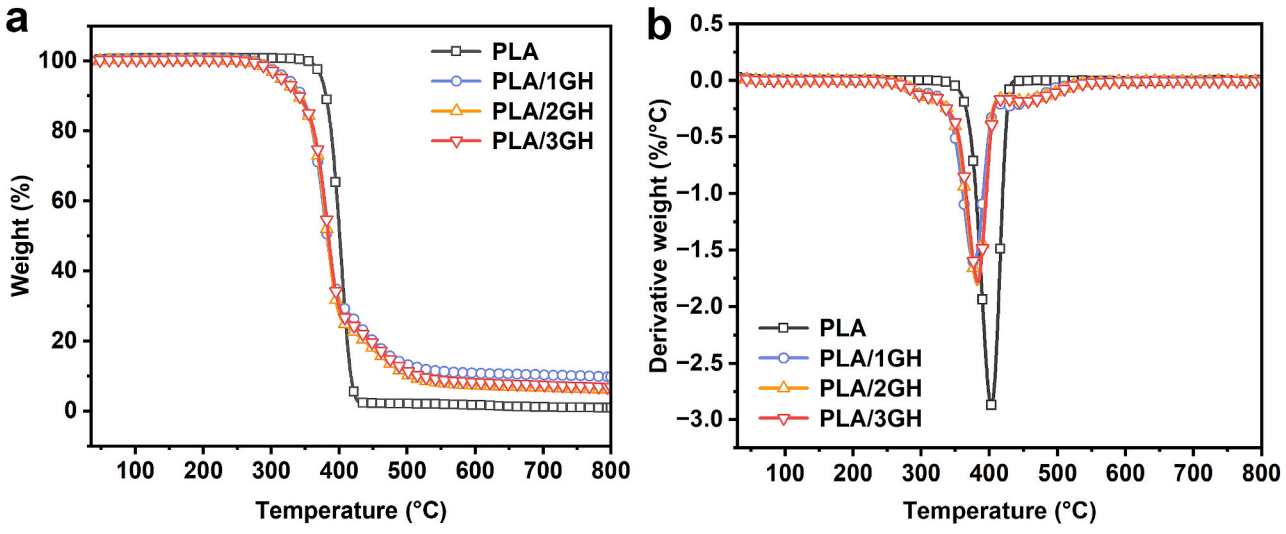

Fig. 3. (a) TG and (b) DTG plots of PLA and PLA/GH composites in N_2 conditions.

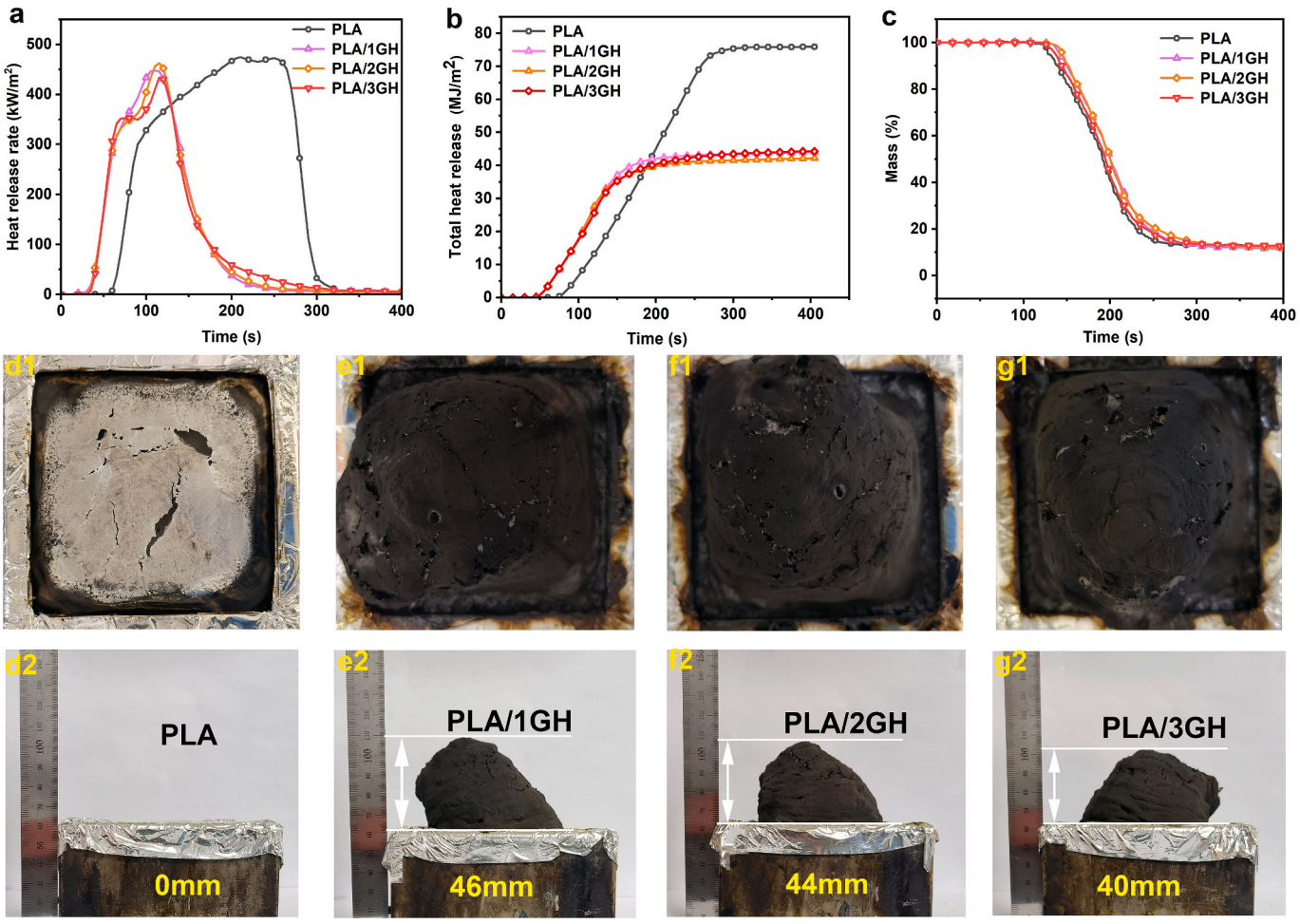

Fig. 4. (a) Heat release rate; (b) total heat release; and (c) mass loss plots of PLA and its composites; and digital photographs of (d1, d2) PLA, (e1, e2) PLA/1GH, (f1, f2) PLA/2GH, and (g1, g2) PLA/3GH chars after cone calorimetry.

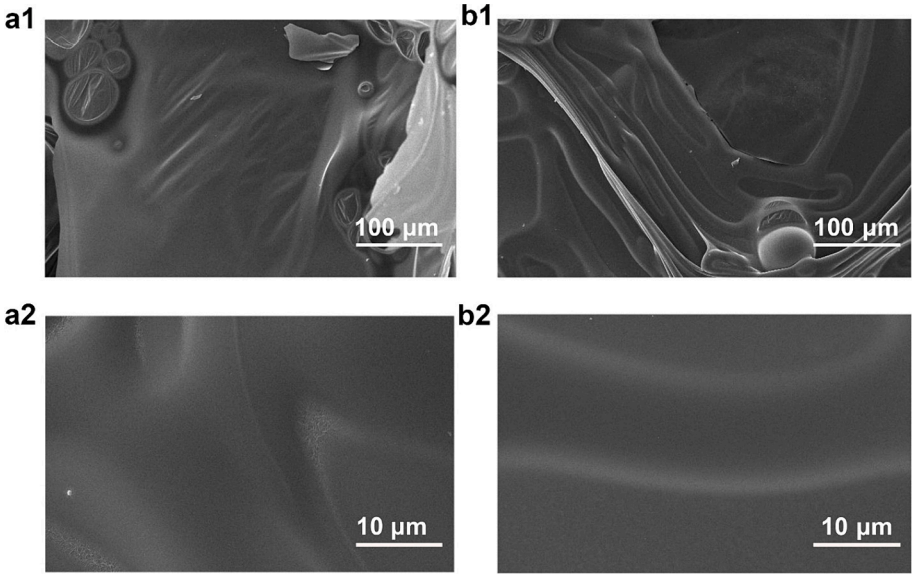

Fig. 5. SEM images of (a1, a2) PLA/2GH, and (b1, b2) PLA/3GH char layers after cone calorimetry tests.

structure, respectively. A low area ratio of D peak to G peak (I_D/I_G) implies high graphitization and good thermal stability [50]. Compared with PLA char, the PLA/GH chars display lower I_D/I_G values, indicative of higher degrees of graphitization (see Fig. 6a-c). Thus, the introduction of MDI and DHDP contributes to promoting the carbonization of the PLA matrix, further demonstrating the positive influence of MDI and DHDP

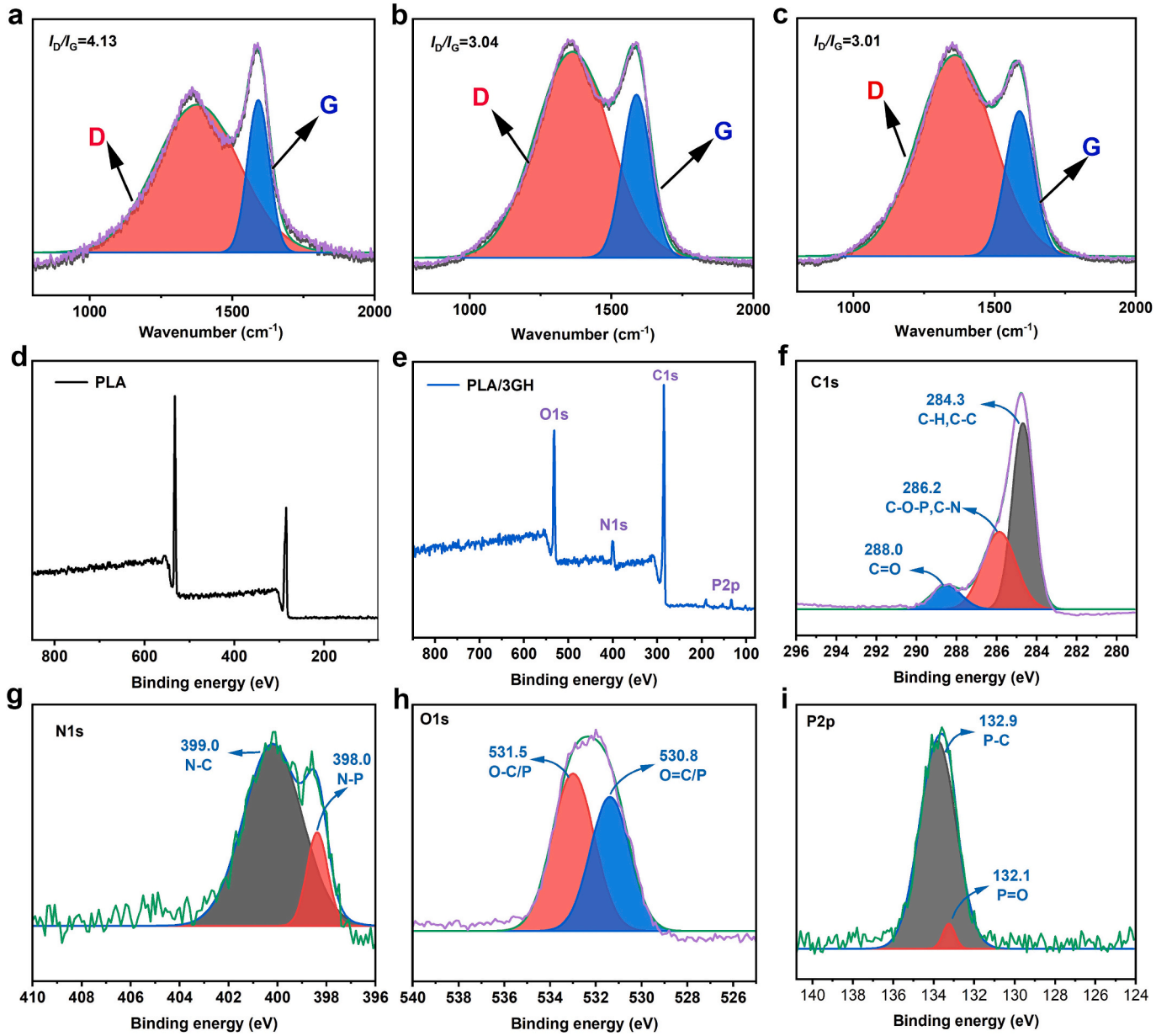

Fig. 6. Raman spectra of the residual chars for (a) PLA, (b) PLA/2GH and (c) PLA/3GH after cone calorimetry tests; XPS survey spectra of (d) PLA, and (e) PLA/3GH chars; and high-resolution (f) C1s, (g) N1s, (h) O1s, and (i) P2p spectra of PLA/3GH residue.

in enhancing the char structure during combustion.

The chemical structures of PLA and PLA/3GH char layers were studied by XPS (see Fig. 6d-i and Table S6). In comparison to PLA char, new elements (phosphorus and nitrogen) appear in the PLA/3GH residue (see Fig. 6d and e). In Fig. 6f, the peak at 288.0 eV is attributed to C═O bond, that at 286.2 eV belongs to C-O-P/C-N bonds, and that at 284.3 eV is assigned to C-H/C-C bonds. In Fig. 6g, the N—C peak can be detected at 399.0 eV, and the N—P peak appears 398.0 eV [51]. The peaks at 531.5 and 530.8 eV in the O1s spectrum belong to O-C/P and O=C/P bonds (see Fig. 6h) [52], and those at 132.9 and 132.1 eV in the P2p spectrum belong to P—O and P═O structures (see Fig. 6i) [53]. Moreover, the N and P contents of PLA/3GH residue are 7.21 % and 1.92 %, respectively, and the carbon content is increased from 65.69 % of PLA char to 72.16 %. This suggests that both MDI and DHDP participate in the carbonization during combustion, enabling more carbon-derived fragments to remain in the char layer, thus enhancing the flame retardancy of PLA composite [54].

3.6. TGA-IR analysis

The TGA-IR tests of PLA and PLA/3GH in N_2 condition were undertaken, with the spectra shown in Fig. 7. The major degradation products of PLA and PLA/3GH are aliphatic ester (1119 cm^{-1}), C—O group (1245 cm^{-1}), C—H group (1375 cm^{-1}), carbonyl compounds (1762 cm^{-1}), carbon monoxide (2181 cm^{-1}), carbon dioxide (2356 cm^{-1}), hydrocarbons (2738 cm^{-1}), and water (3582 cm^{-1}) (see Fig. 7a, b and e) [55–57]. Compared with PLA, the peak intensities of the decomposition products of PLA/3GH are significantly reduced (see Fig. 7a-d), suggesting that the thermal degradation of the composite is retarded due to the existence of MDI and DHDP. Notably, the peak intensity around 1245 cm^{-1} in the spectrum of PLA/3GH is much higher than that in the spectrum of PLA (see Fig. 7e), which may be due to the combination of P═O and C═O peaks. It indicates that DHDP may decompose to release P-containing radicals into the gas phase under heating. The phosphorus-derived radicals can trap the active radicals generated by the PLA matrix to reduce the burning degree [28,57].

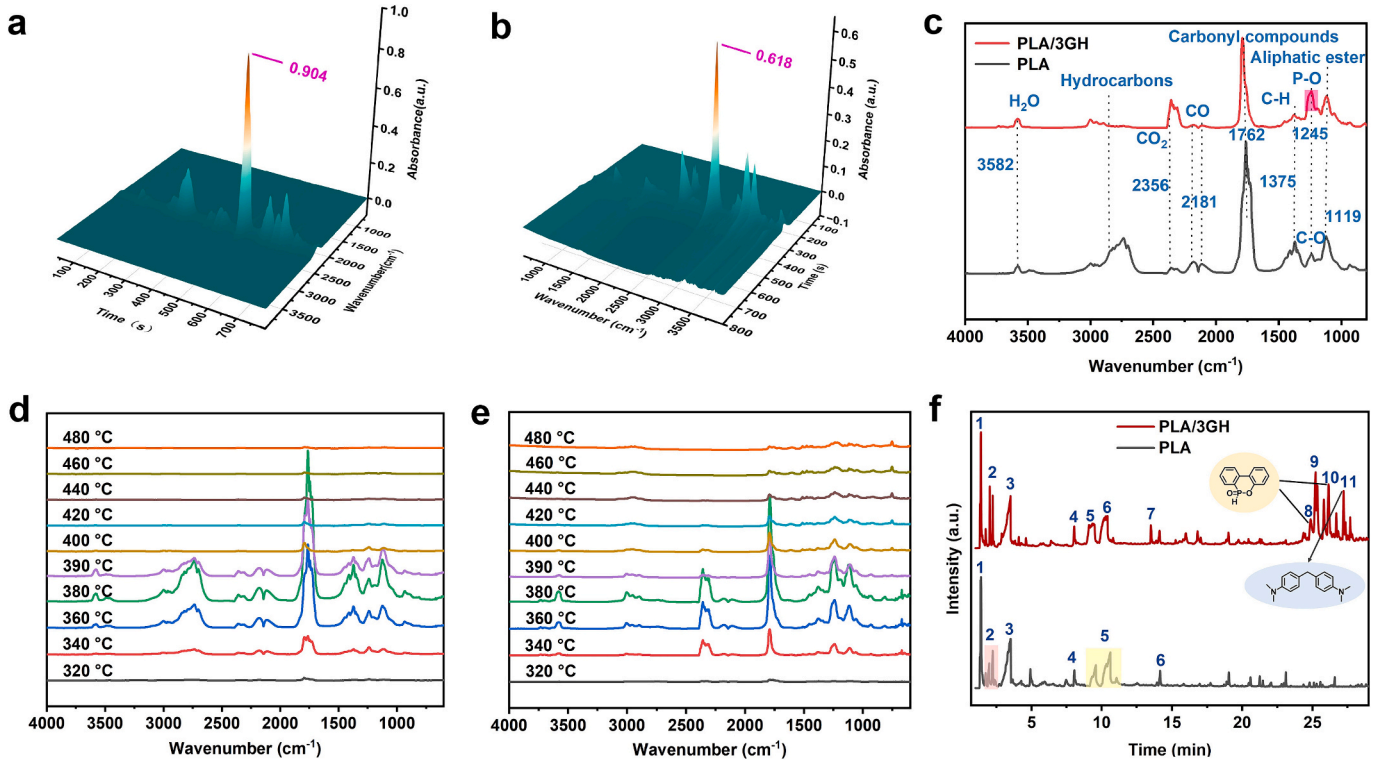

Fig. 7. 3D IR spectra of (a) PLA and (b) PLA/3GH decomposition products; (c) IR spectra of PLA and PLA/3GH decomposition products at T_{max}; IR spectra of (d) PLA and (e) PLA/3GH decomposition products at different temperatures; and (f) total ion chromatograms of the pyrolysis fragments for PLA and PLA/3GH obtained from Py-GC/MS tests.

3.7. Py-GC/MS analysis

To gain more insight into the gas-phase flame-retardant mechanism of PLA/GH composites, the pyrolysis behaviors of PLA and PLA/3GH at 500 °C were analyzed by using Py-GC/MS. Fig. 7f shows the total ion chromatograms of the pyrolysis fragments of PLA and PLA/3GH. The main pyrolysis products of PLA and PLA/3GH are consistent (see Tables S7 and S8). It is worth noting that the PLA/3GH composite pyrolyzes to produce the DHDP- and MDI-derived fragments when the retention time exceeds 15 min (see Fig. 7f and Table S7 and S8). Such result further confirms that PLA/3GH will degrade to release DHDP- and MDI-derived fragments into gas phase during combustion, which may further decompose to generate phosphorus-containing radicals with a quenching effect and nitrogen-containing fragments with a diluting effect, thus reducing the gas-phase combustion degree.

In summary, the significantly improved fire safety of PLA/GH composites is mainly due to DHDP and MDI promoting the generation of an expanded char layer on the matrix surface and reducing the gas-phase burning degree by quenching and diluting high-energy radicals in the combustion procedure (see Fig. S3).

4. Conclusions

To enhance both toughness and flame retardancy of PLA, we covalently introduce the PU chain segments into the PLA matrix by the well-designed interphase reaction between PLA, DHDP and MDI. Both DHDP and MDI are commercially available, and the preparation of PLA/GH composites does not involve any solvents. Due to the formation of rigid PU segment, the PLA/2GH composite displays 14.4 %, 23.4 % and 4.9 % enhancements in the elongation at break, impact strength, and flexural strength relative to those of PLA, indicative of the well-preserved mechanical robustness and enhanced toughness. Introducing MDI and DHDP also brings about significantly improved flame retardancy. All PLA/GH bioplastics achieve the UL-94 V-0 level, and the LOI of PLA/3GH reaches 30.4 %. Meanwhile, the PHRR, THR and AEHC of PLA/3GH respectively reduces by 8.6 %, 43.7 %, and 33.7 % relative to those of PLA. The formation of expanded char layer and suppressed gas-phase burning reaction are responsible for the enhanced fire safety of PLA/GH composites. This work reveals a facile yet effective method to prepare flame-retardant, mechanically-strong and tough PLA composites *via in-situ* constructing P/N-containing PU chain segment within the PLA matrix, which contributes to the sustainable development.

CRediT authorship contribution statement

Zimeng Zhang: Writing – original draft, Investigation, Data curation. **Siqi Huo:** Writing – review & editing, Project administration, Methodology, Conceptualization. **Lingfeng Yu:** Investigation, Data curation. **Guofeng Ye:** Investigation. **Cheng Wang:** Investigation. **Qi Zhang:** Supervision. **Zhitian Liu:** Supervision, Project administration.

Declaration of competing interest

The authors declare that they have no known competing financial interests or personal relationships that could have appeared to influence the work reported in this paper.

Data availability

Data will be made available on request.

Acknowledgments

This work was funded by the Australian Research Council Discovery Early Career Researcher Award (DE230100616), the Foundation for Outstanding Youth Innovative Research Groups of Higher Education Institution in Hubei Province (T201706), and the Foundation for Innovative Research Groups of Hubei Natural Science Foundation of China

(2017CFA009).

Appendix A. Supplementary data

Supplementary data to this article can be found online at https://doi.org/10.1016/j.ijbiomac.2024.130806.

References

[1] Y. Yang, L.S. Zhang, Z. Xiong, Z.B. Tang, R.Y. Zhang, J. Zhu, Research progress in the heat resistance, toughening and filling modification of PLA, Sci. China Chem. 59 (11) (2016) 1355–1368, https://doi.org/10.1007/s11426-016-0222-7.

[2] X.W. Cao, J.S. Huang, Z.J. Tang, Y.Z. Tong, A.C.Y. Yuen, W.J. Zhao, Q.L. Huang, R. K.Y. Li, W. Wu, Self-assembled biobased chitosan hybrid carrying N/P/B elements for polylactide with enhanced fire safety and mechanical properties, Int. J. Biol. Macromol. 236 (2023), https://doi.org/10.1016/j.ijbiomac.2023.123947 (123947-123947).

[3] Y.J. Xue, T.C. Zhang, L.F. Tian, J.B. Feng, F. Song, Z. Pan, M. Zhang, Y.H. Zhou, P. A. Song, A molecularly engineered bioderived polyphosphonate containing Schiff base towards fire-retardant PLA with enhanced crystallinity and mechanical properties, Chem. Eng. J. 472 (2023) 144986, https://doi.org/10.1016/j.cej.2023.144986.

[4] Y.R. Sun, B. Yu, Y. Liu, J.B. Yan, Z.X. Xu, B. Cheng, F.L. Huang, J. Wang, Bio-inspired surface manipulation of halloysite nanotubes for high-performance flame retardant polylactic acid nanocomposites, Nano Res. (2023) 1–12, https://doi.org/10.1007/s12274-023-6050-y.

[5] X. Zhao, J. Yu, X. Wang, Z. Huang, W. Zhou, S. Peng, Strong synergistic toughening and compatibilization enhancement of carbon nanotubes and multi-functional epoxy compatibi- lizer in high toughened polylactic acid (PLA)/poly (butylene adipate-co-terephthalate) (PBAT) blends, Int. J. Biol. Macromol. 250 (2023), https://doi.org/10.1016/j.ijbiomac.2023.126204 (126204-126204).

[6] T.T. Bai, B. Zhu, H. Liu, Y.M. Wang, G. Song, C.T. Liu, C.Y. Shen, Biodegradable poly(lactic acid) nanocomposites reinforced and toughened by carbon nanotubes/clay hybrids, Int. J. Biol. Macromol. 151 (2020) 628–634, https://doi.org/10.1016/j.ijbiomac.2020.02.209.

[7] S.P. Qian, K.C. Sheng, PLA toughened by bamboo cellulose nanowhiskers: role of silane compatibilization on the PLA bionanocomposite properties, Compos. Sci. Technol. 148 (2017) 59–69, https://doi.org/10.1016/j.compscitech.2017.05.020.

[8] S.P. Qian, K.C. Sheng, K. Yu, L.Q. Xu, C.A.F. Lopez, Improved properties of PLA biocomposites toughened with bamboo cellulose nanowhiskers through silane modification, J. Mater. Sci. 53 (15) (2018) 10920–10932, https://doi.org/10.1007/s10853-018-2377-2.

[9] K.C. Sheng, S. Zhang, S.P. Qian, C.A.F. Lopez, High-toughness PLA/bamboo cellulose nanowhiskers bionanocomposite, strengthened with silylated ultrafine bamboo-char, Compos. Part B-Eng. 165 (2019) 174–182, https://doi.org/10.1016/j.compositesb.2018.11.139.

[10] T. Zhao, J.S. Yu, H.W. Pan, Y. Zhao, Q.X. Zhang, X.Y. Yu, J.J. Bian, L.J. Han, H. L. Zhang, Super-tough polylactic acid (PLA)/poly(butylene succinate) (PBS) materials prepared through reactive blending with epoxy-functionalized PMMA-GMA copolymer, Int. J. Biol. Macromol. 251 (2023), https://doi.org/10.1016/j.ijbiomac.2023.126150 (126150-126150).

[11] K. Chen, C. Zhou, L. Yao, M.F. Jing, C.T. Liu, C.Y. Shen, Y.M. Wang, Phase morphology, rheological behavior and mechanical properties of supertough biobased poly(lactic acid) reactive ternary blends, Int. J. Biol. Macromol. 253 (2023), https://doi.org/10.1016/j.ijbiomac.2023.127079 (127079-127079).

[12] T.T. Chen, Y.C. Wu, J.H. Qiu, M.G. Fei, R.H. Qiu, W.D. Liu, Interfacial compatibiliza- tion via in-situ polymerization of epoxidized soybean oil for bamboo fibers reinforced poly(lactic acid) biocomposites, Compos. Part A-Appl. Sci. Manuf. 138 (2020) 106066, https://doi.org/10.1016/j.compositesa.2020.106066.

[13] X. Song, C. Zhang, Y. Yang, Y. Weng, Effect of oligomers from epoxidized soybean oil and sebacic acid on the toughness of polylactic acid/bamboo fiber composites, J. Appl. Polym. Sci. 139 (5) (2021) 51583, https://doi.org/10.1002/app.51583.

[14] S. Mahmud, Y. Long, M. Abu Taher, Z. Xiong, R.Y. Zhang, J. Zhu, Toughening polylactide by direct blending of cellulose nanocrystals and epoxidized soybean oil, J. Appl. Polym. Sci. 136 (46) (2019) 48221, https://doi.org/10.1002/app.48221.

[15] Y.B. Liu, Z. Xu, Z.M. Zhang, R.Y. Bao, M.B. Yang, W. Yang, Blowing tough polylactide film enabled by the construction of covalent adaptive networks with epoxidized soybean oil as dynamic crosslinks, Green Chem. 25 (13) (2023) 5182–5194, https://doi.org/10.1039/d3gc00999h.

[16] T.H. Zhao, W.Q. Yuan, Y.D. Li, Y.X. Weng, J.B. Zeng, Relating chemical structure to toughness via morphology control in fully sustainable sebacic acid cured epoxidized soybean oil toughened polylactide blends, Macromolecules 51 (5) (2018) 2027–2037, https://doi.org/10.1021/acs.macromol.8b00103.

[17] S. Wang, B.D. Liu, Y.Y. Qin, H.G. Guo, Effects of processing conditions and plasticizing-reinforcing modification on the crystallization and physical properties of PLA films, Membranes 11 (8) (2021), https://doi.org/10.3390/membranes11080640 (640-640).

[18] W.D. Liu, J.H. Qiu, M.E. Fei, R.H. Qiu, E. Sakai, Manufacturing of thermally remoldable blends from epoxidized soybean oil and poly(lactic acid) via dynamic cross-linking in a twin-screw extruder, Ind. Eng. Chem. Res. 57 (22) (2018) 7516–7524, https://doi.org/10.1021/acs.iecr.8b01189.

[19] X.J. Chen, R.Q. Zhang, Y.X. Mao, L.L. Zhong, P.Y. Lin, Q.Z. Deng, B.T. Zheng, H. Shen, Z.M. Feng, H.G. Zhang, Development of a toughened and antibacterial Poly(lactide acid) (PLA) with preserved strength by elemental sulfur-based bio-renewable dynamically crosslinked elastomers, Chem. Eng. J. 467 (2023) 143419, https://doi.org/10.1016/j.cej.2023.143419.

[20] M. Ma, L. Xu, K. Liu, S. Chen, H. He, Y. Shi, X. Wang, Effect of triphenyl phosphite as a reactive compatibilizer on the properties of poly(L-lactic acid)/poly(butylene succinate) blends, J. Appl. Polym. Sci. 137 (18) (2019) 48646, https://doi.org/10.1002/app.48646.

[21] H.Z. Liu, N. Chen, P.J. Shan, P.A. Song, X.Y. Liu, J.Z. Chen, Toward fully bio-based and supertough PLA blends via in situ formation of cross-linked biopolyamide continuity network, Macromolecules 52 (21) (2019) 8415–8429, https://doi.org/10.1021/acs.macromol.9b01398.

[22] X.D. Xu, J.F. Dai, Z.W. Ma, L.N. Liu, X.H. Zhang, H.Z. Liu, L.C. Tang, G.B. Huang, H. Wang, P.A. Song, Manipulating interphase reactions for mechanically robust, flame-retardant and sustainable polylactide biocomposites, Compos. Part B-Eng. 190 (2020), https://doi.org/10.1016/j.compositesb.2020.107930 (107930-107930).

[23] W.D. Liu, J.H. Qiu, T.T. Chen, M.G. Fei, R.H. Qiu, E. Sakai, Regulating tannic acid-crosslinked epoxidized soybean oil oligomers for strengthening and toughening bamboo fibers-reinforced poly(lactic acid) biocomposites, Compos. Sci. Technol. 181 (2019), https://doi.org/10.1016/j.compscitech.2019.107709 (107709-107709).

[24] Q.Y. Ge, Q. Dou, Preparation of supertough polylactide/polybutylene succinate/epoxidized soybean oil bio-blends by chain extension, ACS Sustain. Chem. Eng. 11 (26) (2023) 9620–9629, https://doi.org/10.1021/acssuschemeng.3c01042.

[25] M. Ma, K. Liu, H.M. Zheng, S. Chen, B.Z. Wu, Y.Q. Shi, X. Wang, Effect of the composition and degree of crosslinking on the properties of poly (L-lactic acid)/crosslinked polyurethane blends, Polym. Int. 67 (9) (2018) 1221–1228, https://doi.org/10.1002/pi.5626.

[26] W. Yang, Y. Zhu, T. Liu, D. Puglia, J.M. Kenny, P. Xu, R. Zhang, P. Ma, Multiple structure reconstruction by dual dynamic crosslinking strategy inducing self-reinforcing and toughening the polyurethane/nanocellulose elastomers, Adv. Funct. Mater. 33 (12) (2023) 2213294, https://doi.org/10.1002/adfm.202213294.

[27] H.Z. Liu, N. Chen, C.Q. Peng, S. Zhang, T. Liu, P.A. Song, G.L. Zhong, H. Liu, Diisocyanate-induced dynamic vulcanization of difunctional fatty acids toward mechanically robust PLA blends with enhanced luminescence emission, Macromolecules 55 (17) (2022) 7695–7710, https://doi.org/10.1021/acs.macromol.2c00674.

[28] J.S. Wang, X. Chen, J. Wang, S. Yang, K.W. Chen, L. Zhu, S.Q. Huo, P.A. Song, H. Wang, High-performance, intrinsically fire-safe, single-component epoxy resins and carbon fiber reinforced epoxy composites based on two phosphorus-derived imidazoliums, Polym. Degrad. Stab. 208 (2023) 110261, https://doi.org/10.1016/j.polymdegradstab.2023.110261.

[29] L. Liu, Y. Xu, Y. Pan, M. Xu, Y. Di, B. Li, Facile synthesis of an efficient phosphonamide flame retardant for simultaneous enhancement of fire safety and crystallization rate of poly (lactic acid), Chem. Eng. J. 421 (2021) 127761, https://doi.org/10.1016/j.cej.2020.127761.

[30] Y.J. Xue, J.Y. Lin, T. Wan, Y.L. Luo, Z.W. Ma, Y.H. Zhou, B.T. Tuten, M. Zhang, X. Y. Tao, P.A. Song, Stretchable, ultratough, and intrinsically self-extinguishing elastomers with desirable recyclability, Adv. Sci. 10 (9) (2023) 2207268, https://doi.org/10.1002/advs.202207268.

[31] W.F. Liu, C. Fang, S.Y. Wang, J.H. Huang, X.Q. Qiu, High-performance lignin-containing polyurethane elastomers with dynamic covalent polymer networks, Macromolecules 52 (17) (2019) 6474–6484, https://doi.org/10.1021/acs.macromol.9b01413.

[32] H. Zhang, J. Shu, Z. Liu, J. Wu, High-performance crack-resistant elastomer with tunable "J-Shaped" stress–strain behavior inspired by the brown pelican, ACS Appl. Mater. Interfaces 14 (19) (2022) 22489–22496, https://doi.org/10.1021/acsami.2c06646.

[33] Y. Zhang, J. Jing, T. Liu, L.D. Xi, T. Sai, S.Y. Ran, Z.P. Fang, S.Q. Huo, P.G. Song, A molecularly engineered bioderived polyphosphate for enhanced flame retardant, UV-blocking and mechanical properties of poly(lactic acid), Chem. Eng. J. 411 (2021) 128493, https://doi.org/10.1016/j.cej.2021.128493.

[34] M. Zhang, Y. Wang, J. Huang, D. Wang, T. Li, S. Wang, W. Dong, Phytic acid–based flame retardant and its application to poly(lactic acid) composites, New J. Chem. 47 (42) (2023) 19494–19503, https://doi.org/10.1039/d3nj03460g.

[35] Z.L. Jiang, M. Ma, X.P. Wang, S. Chen, Y.Q. Shi, H.W. He, X. Wang, Toward flame-retardant and toughened poly(lactic acid)/cross-linked polyurethane blends via the interfacial reaction with the modified bio-based flame retardants, Int. J. Biol. Macromol. 251 (2023) 126206, https://doi.org/10.1016/j.ijbiomac.2023.126206.

[36] H. Cheng, Y. Wu, W. Hsu, F. Lin, S. Wang, J. Zeng, Q. Zhu, L. Song, Green and economic flame retardant prepared by the one-step method for polylactic acid, Int. J. Biol. Macromol. 253 (2023) 127291, https://doi.org/10.1016/j.ijbiomac.2023.127291.

[37] L.F. Yu, S.Q. Huo, C. Wang, G.F. Ye, P.A. Song, J.B. Feng, Z.P. Fang, H. Wang, Z. T. Liu, Flame-retardant poly(L-lactic acid) with enhanced UV protection and well-preserved mechanical properties by a furan-containing polyphosphoramide, Int. J. Biol. Macromol. 234 (2023) 123707, https://doi.org/10.1016/j.ijbiomac.2023.123707.

[38] M.J. Cui, J. Li, X.D. Chen, W. Hong, Y. Chen, J. Xiang, J. Yan, H.J. Fan, A halogen-free, flame retardant, waterborne polyurethane coating based on the synergistic effect of phosphorus and silicon, Prog. Org. Coat. 158 (2021) 106359, https://doi.org/10.1016/j.porgcoat.2021.106359.

[39] J. Wang, S.Y. Zhou, Y. Qu, B. Yang, Q. Zhang, Y. Lin, G.P. Lu, Modified Gallic acids as both reactive flame retardants and cross-linkers for the fabrication of flame-retardant polyurethane elastomers, ChemistrySelect 8 (39) (2023) e202302496, https://doi.org/10.1002/slct.202302496.

[40] M.A. Elsawy, K.H. Kim, J.W. Park, A. Deep, Hydrolytic degradation of polylactic acid (PLA) and its composites, Renew. Sust. Energ. Rev. 79 (2017) 1346–1352, https://doi.org/10.1016/j.rser. 2017.05.143.
[41] Y.Q. Shi, Z.X. Wang, C. Liu, H.R. Wang, J. Guo, L.B. Fu, Y.Z. Feng, L.C. Wang, F. Q. Yang, M.H. Liu, Engineering titanium carbide ultra-thin nanosheets for enhanced fire safety of intumescent flame retardant polylactic acid, Compos. Part B-Eng. 236 (2022) 109792, https://doi.org/10.1016/j.compositesb.2022.109792.
[42] X. Zhao, Z. Ding, Q. Lin, S. Peng, P. Fang, Toughening of polylactide via in situ formation of polyurethane crosslinked elastomer during reactive blending, J. Appl. Polym. Sci. 134 (2) (2016) 44383, https://doi.org/10.1002/app.44383.
[43] P. Zhu, S. Liu, R. Feng, L. Yang, L. Liu, Y. Huang, J. Li, Rigid epoxy microspheres reinforced and toughened polylactic acid through enhancement of interfacial reactivity, Compos. Sci. Technol. 232 (2023) 109888, https://doi.org/10.1016/j.compscitech.2022.109888.
[44] G. Ye, S. Huo, C. Wang, Q. Shi, Z. Liu, H. Wang, One-step and green synthesis of a bio-based high-efficiency flame retardant for poly (lactic acid), Polym. Degrad. Stab. 192 (2021) 109696, https://doi.org/10.1016/j.polymdegradstab.2021.109696.
[45] Q. Yang, J. Wang, X. Chen, S. Yang, S. Huo, Q. Chen, P. Guo, X. Wang, F. Liu, W. Chen, P. Song, H. Wang, A phosphorus-containing tertiary amine hardener enabled flame retardant, heat resistant and mechanically strong yet tough epoxy resins, Chem. Eng. J. 468 (2023) 143811, https://doi.org/10.1016/j.cej.2023.143811.
[46] J. Ren, S. Huo, G. Huang, T. Wang, J. Feng, W. Chen, S. Xiao, P. Song, A novel P/Ni-doped g-C3N4 nanosheets for improving mechanical, thermal and flame-retardant properties of acrylonitrile–butadienestyrene resin, Chem. Eng. J. 452 (2023) 139196, https://doi.org/10.1016/j.cej.2022.139196.
[47] P. Zhao, W.H. Rao, H.Q. Luo, L. Wang, Y.L. Liu, C.B. Yu, Novel organophosphorus compound with amine groups towards self-extinguishing epoxy resins at low loading, Mater. Des. 193 (2020) 108838, https://doi.org/10.1016/j.matdes.2020.108838.
[48] J. Zhang, Z. Li, L. Zhang, Y. Yang, D.-Y. Wang, Green synthesis of biomass phytic acid-functionalized UiO-66-NH2 hierarchical hybrids toward fire safety of epoxy resin, ACS Sustain. Chem. Eng. 8 (2) (2019) 994–1003, https://doi.org/10.1021/acssuschemeng.9b05658.
[49] S.Q. Huo, P.A. Song, B. Yu, S.Y. Ran, V.S. Chevali, L. Liu, Z.P. Fang, H. Wang, Phosphorus-containing flame retardant epoxy thermosets: recent advances and future perspectives, Prog. Polym. Sci. 114 (2021) 101366, https://doi.org/10.1016/j.progpolymsci.2021.101366.
[50] W. Sun, Y. Sun, Growth of biobased flakes on the surface and within interlayer of metakaolinite to enhance the fire safety and mechanical properties of intumescent flame-retardant polyurea composites, Chem. Eng. J. 450 (2022) 138350, https://doi.org/10.1016/j.cej.2022. 138350.
[51] X.B. Ma, N.J. Wu, P.B. Liu, H.L. Cui, Fabrication of highly efficient phenylphosphorylated chitosan bio-based flame retardants for flammable PLA biomaterial, Carbohydr. Polym. 287 (2022) 119317, https://doi.org/10.1016/j.carbpol.2022.119317.
[52] S.M. Seraji, H.L. Gan, S. Issazadeh, R.J. Varley, Investigation of the dual polymerization of rapid curing organophosphorous modified epoxy/amine resins and subsequent flame retardancy, Macromol. Chem. Phys. 222 (7) (2021) 2000342, https://doi.org/10.1002/macp.2020 00342.
[53] T. Suparanon, W. Phetwarotai, Fire-extinguishing characteristics and flame retardant mechanism of polylactide foams: influence of tricresyl phosphate combined with natural flame retardant, Int. J. Biol. Macromol. 158 (2020) 1090–1101, https://doi.org/10.1016/j.ijbiomac.2020. 04.131.
[54] Y.-J. Xu, X.-H. Shi, J.-H. Lu, M. Qi, D.-M. Guo, L. Chen, Y.-Z. Wang, Novel phosphorus-containing imidazolium as hardener for epoxy resin aiming at controllable latent curing behavior and flame retardancy, Compos. Part B-Eng. 184 (2020) 107673, https://doi.org/10.1016/j.compositesb.2019.107673.
[55] X.G. Wang, S.H. Wang, W.J. Wang, H.F. Li, X.D. Liu, X.Y. Gu, S. Bourbigot, Z. W. Wang, J. Sun, S. Zhang, The flammability and mechanical properties of poly (lactic acid) composites containing Ni-MOF nanosheets with polyhydroxy groups, Compos. Part B-Eng. 183 (2020) 107568, https://doi.org/10.1016/j.compositesb.2019.107568.
[56] L. Zhang, Z. Li, Y.T. Pan, A.P. Yáñez, S. Hu, X.Q. Zhang, R. Wang, D.Y. Wang, Polydopamine induced natural fiber surface functionalization: a way towards flame retardancy of flax/poly(lactic acid) biocomposites, Compos. Part B-Eng. 154 (2018) 56–63, https://doi.org/10.1016/j.compositesb.2018.07.037.
[57] J. He, T. Yu, Y. Li, Biodegradable thermoset poly(lactic acid) resin containing phosphorus: flame retardancy, mechanical properties and its soil degradation behavior, Int. J. Biol. Macromol. 235 (2023) 123737, https://doi.org/10.1016/j.ijbiomac.2023.123737.